ELSEVIER

Coordination Chemistry Reviews
178–180 (1998) 1753–1783

COORDINATION CHEMISTRY REVIEWS

Structure–activity relationships in catalysis by metals: some aspects of particle size, bimetallic and supports effects

Bernard Coq *, François Figueras [1]

Laboratoire de Matériaux Catalytiques et Catalyse en Chimie Organique, UMR 5618 ENSCM-CNRS, 8, Rue de l'Ecole Normale, 34296 Montpellier, France

Received 24 October 1997; received in revised form 22 January 1998; accepted 27 January 1998

Contents

* Corresponding author.
[1] Present address: Institut de Recherche sur la Catalyse, 2 Avenue Albert Einstein, 69626 Villeurbanne, France.

PII S0010-8545(98)00058-7

Abstract

Some aspects of particle size, bimetallic formulation and metal–support interaction on the catalytic properties of supported metal catalysts in the hydrogenolysis of C–C and C–halogen bonds, and the hydrogenation of nitroaromatics and α,β-unsaturated aldehydes are presented. The influences of these parameters on the kinetics, the mechanism, the nature of adsorbed intermediates and the consequences on turnover frequency and selectivity are highlighted. It is shown, in particular, how the topology of the active site, and the coordination of the metal atoms, can determine the nature of the surface intermediates and, *in fine*, the orientation of the reaction. This is a review mainly based on the researches carried out over two decades in the "Laboratoire de Matériaux Catalytiques et Catalyse en Chimie Organique, UMR 5618 ENSCM-CNRS".

Keywords: Heterogeneous catalysis; Supported metals; Dimetallic catalysts; Metal-support interaction

1. Introduction

Heterogeneous catalysis is a branch of kinetics and intervenes in more than 80% of the processes for producing chemicals. The research in heterogeneous catalysis aims at the design of novel, less energy consuming, intrinsically safer and cleaner catalytic processes. This means less waste production and fewer by-products. As an example, minimization of wastes and by-products can be reached by the replacement of liquid acids by solid acids. It can also be achieved by developing very-selective catalysts. This was particularly true in catalysis by metals with the multimetallic formulations in the reforming of naphtha, and current work on the selective hydrogenation in petrochemical processes has the same aim.

The fulfillment of these objectives requires fundamental and applied researches for (i) the discovery of novel or improved catalyst formulations and (ii) a better understanding of physical and chemical phenomena underlying the catalytic transformation. These researches have shown that a large number of reactions exists for which the rate per unit of catalyst area depends on the superficial structure of a catalyst with a given chemical composition. This general concept of "structure-sensitivity" was particularly fruitful in the field of catalysis by metals. Depending on whether the turnover frequency (TOF), or rate per unit surface area or per accessible metal atom, is affected or not by the metallic structure, the reactions have been termed as either "facile" or "demanding" [1], or later on by the terms structure-insensitive or structure-sensitive [2].

The first to recognize this concept was Taylor [3], in 1925, who said: "…the amount of surface which is catalytically active is determined by the reaction catalyzed. There will be all extremes between the case in which all the atoms in the surface are active and that in which relatively few are so active…".

In the broad sense, we mean by superficial metallic structure the coordination number between the active metal atoms which can be modified [4]: (i) by exposing different crystallographic planes at the surface and making them imperfect by means of steps and kinks; (ii) by varying particle size in the critical range between 1 and

5 nm; (iii) by diluting the active surface by a second inactive metal, in the case of alloys or bimetallic catalysts; (iv) by induction of a strong metal–support interaction with some supports. Each of these situations has been the subject of reviews dealing with (i) particle-size and plane-structure sensitivities [5], (ii) ensemble-size sensitivity [6] and (iii) metal–support interaction [7].

Although this separation somehow seems arbitrary, and could be criticized, there is, more or less, a general agreement in explaining these structure–activity relationships with the help of geometric and electronic effects (*vide infra*).

However, we have to take care with the simple view of a geometric basis for explaining structure-sensitivity. There is the possibility, under high temperature conditions or very reactive atmospheres, that surface mobility smooths out geometric and structural features on small particles. This concept of a flexible surface, mainly revealed by Somorjai [8], and the correlation between reactivity and restructuring ability appears extremely puzzling, but fruitful.

Another point which needs careful consideration is kinetic measurements. The use of a single set of reaction conditions, giving a single rate measurement, is less significant, as the relative activities of two catalysts can be very dependent on the reactant pressures and temperatures used [9]. If a single set of reaction conditions is being used, it is better, if the reaction allows, to compare the catalysts on the base of the selectivity patterns. Moreover, it is never sure that TOF can be determined and assigned unequivocally to the chemical processes, and heat and mass transfer limitations might affect the experiments. In this respect, it is also preferable to select a molecule which can react along different parallel paths and follow the changes of selectivity with the superficial metallic structure.

Finally, it is of prime importance to prepare and study well-defined model catalysts to derive valuable conclusions, as stated by Bond [10] "…A common fault is to use poorly controlled methods to prepare a small amount of catalyst, and to spend weeks if not months in studying it…".

For two decades we have been studying this field of catalysis by metals, and this is a review of selected work we have done on hydrogenation and hydrogenolysis reactions on supported metal catalysts. After a short presentation of the basic concepts developed to interpret the structure–activity relationships, we will present studies dealing with the hydrogenolysis of C–C bonds (alkanes) and C–halogen bonds, and the hydrogenation of halonitrobenzene and of α,β-unsaturated aldehydes. These reactions were carried out on model catalysts composed of Pd, Pt, Rh and Ru supported on Al_2O_3, SiO_2, TiO_2, ZrO_2 and carbon materials. Their preparation will be described briefly.

2. Basic concepts

As mentioned above, the structure–activity relationships are often explained on the basis of electronic and/or geometric effects. However, geometric and electronic influences often cannot be separated as independent parameters. For instance, increasing the size of metallic particles results in an electron bandwidth increase, but the nature of the exposed planes and the topology of the surface sites change

as well. Hence the ambiguity of the electronic and geometric factors is now only of historical interest in catalysis.

2.1. Electronic effect

To be concise, the key point in this model lies in the interaction between the incomplete d-band of the surface sites with the molecular orbitals of reactants and products. Historically, the premises of this concept were suggested by Sabatier [11]. The heat of adsorption of reactants and products, governed by the electronic factors, should be neither too strong nor too weak to give the optimum coverage for species competing at the surface, or for the products to desorb. The synthesis of ammonia (competition between N_2, H_2 and NH_3) and the selective hydrogenation of alkynes (competition between H_2 and alkynes) are good examples of this proposal.

2.2. Geometric effect

The first element of this model lies in the pioneering work of Kobozev [12], and Boronin and Poltorak [13]. They showed that some reactions need more than one surface atom to proceed. Moreover, a specific arrangement between these atoms will even be required to generate the active site [14]. This geometric model was more recently revisited by several authors [15–17], giving it the generic name of the ''ensemble-size'' model. The basic idea is that the rate is a function of the probability of finding an ensemble of n free and neighbor atoms on which the reactive adsorption of the reactant(s), and the further transformations, can occur.

3. Preparation of the catalysts

An ideal preparation of metallic catalysts should result in a homogeneous distribution, within a grain of support, of metallic particles of controlled size. This objective is difficult to reach, since preparation bears some analogies with the synthesis of complex organic molecules: both imply multistep processes, and the quality of the catalyst is determined by that of the worse step. The objective of this work is to consider mainly model catalysts, showing a narrow distribution of particle sizes, on a non-acidic support.

3.1. Preparation of monometallic catalysts of controlled size

The usual methods of catalyst preparation have been reviewed in detail by several recent papers [5,18]. A well-dispersed catalyst can be obtained by the reduction of metallic precursors statistically distributed at the surface of a support. It can be pointed out that both kinetic and thermodynamic factors control this process: a statistical distribution of the precursor from the core to the rim of the catalyst grain requires the use of slow and reversible reactions for the deposition of the metallic precursors. The method we have preferred to use is based on a ligand exchange process between the support and an organometallic precursor [19]. The metal is

deposited by the stoichiometric surface reaction between an acetylacetonate, e.g. $Rh(acac)_3$, and the OH groups of the support, on alumina for instance:

$$Al–OH + Rh(acac)_3 \leftrightarrow Al–O–Rh(acac)_2 + acacH$$

This reaction is reversible and can be displaced by an excess of acetylacetone. The dispersion of Rh species can then be controlled by the dehydroxylation of the support and the addition of acetylacetone.

The reduction in mild conditions yields a well dispersed metal, with a narrow distribution of particles with size below 1 nm (Fig. 1). Since it is well known that water is a vector for sintering, the addition of water in the hydrogen used for reduction allows one to increase the mean size. This method has been applied with success to the synthesis of well dispersed Rh [20], Ru [21–23] and Pt [24,25] catalysts on alumina, zirconia or titania.

3.2. Bimetallic catalysts

To prevent the mixing between an ensemble-size effect and a particle-size effect, it is very important to compare bimetallic catalysts of a very similar particle size. This objective can be achieved by the use of a controlled surface reaction between the metal particles and an organometallic compound [26]. The principle is to react an alkyl metal with the reduced monometallic catalyst in a hydrogen atmosphere. The surface reaction

$$MH + M'Bu_4 \xrightarrow{H_2} (4-x)BuH + MM'Bu_x$$

yields an anchored M′ species. The final solid, which is stable at low temperature, can be reduced to the bimetallic system by hydrogen above 573 K. This procedure has been used to modify M = Pd [27], Rh [28], Ru [22,23,29], Pt [24] with M′ = Sn, Pb, Sb, Al, Ge, Zn, Si. Since the reaction used here is a stoichiometric surface reaction, the same parent sample can be modified by different metals, or with different loadings, and retain a very similar particle size (Fig. 1).

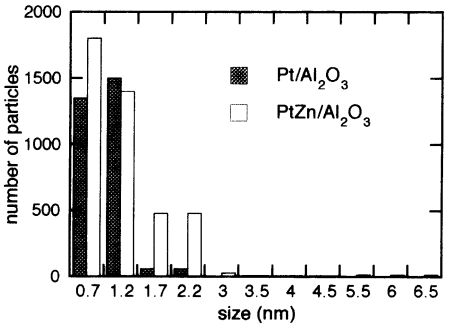

Fig. 1. Distribution of particle sizes for a parent platinum catalyst and the same modified by addition of zinc.

4. Hydrogenolysis of C–C bonds

Over the last four decades, this has been one of the most documented reactions for both practical and fundamental reasons. This reaction is of primary importance in naphtha reforming to increase the octane number. This is usually an unwanted process and the development of improved catalysts has given rise to many academic studies on this subject. C–C hydrogenolysis has long been considered as the archetypal structure-sensitive reaction in both the alkane and cycloalkane series. TOFs do indeed often vary with particle size, but the experimental results show no conformity to any single model. One clear example is the hydrogenolysis of cyclopropane, which is insensitive on Pt catalysts but is highly sensitive to particle size on Ru catalysts [10]. The reasons for the lack of conformity of the results in the literature on hydrogenolysis are not easily discerned [5]. They can be divided within three groups:

(1) the use of catalysts which are not really comparable owing to differences in the broadening of particle size distribution and the presence of poisons or promoters on the support;
(2) the use of different reaction conditions, with respect to the pressure of reactants. There is evidence that the rate law expression can be particle-size dependent [30];
(3) the fact that C–C hydrogenolysis is not a reaction which can be considered as an isolated part of the alkane. Actually, depending on the alkane the C–C bond rupture can occur via a great variety of surface complexes [31–36], which accommodate different degrees of bonding with the surface. This is a key point which is detailed below.

Depending on the nature and the dispersion of the metal, different adsorbed complexes have thus been proposed for C–C hydrogenolysis: 1–2C, 1–3C, 1–4C and 1–5C. These species are illustrated in Scheme 1 for different alkanes. The probability for each species to occur depends on (i) the nature of the alkane, (ii) the nature of the metal, and (iii) the number of free and neighbor surface metal atoms.

However, some general tendencies can be drawn. The 1–2C π-bonded and the 1–3C metallocyclobutane species can occur on a small site (a single atom?). In contrast, the 1–2C, 1–3C and 1–4C multibonded species are favored on the large ensembles of the dense planes.

4.1. Particle-size effect

This topic was recently reviewed in detail by Che and Bennett [5]. In most of the supported metal catalysts the size of the metal particles varies in the critical range between 1 to 10 nm. The first point addresses the question of below what particle size are the metallic properties lost: "how small is a metal?" [37]. The answer is not so simple and depends on the properties we are looking for: the critical size above which the band structure appears is about 2 nm; however, the topology of the surface suffers great changes until 5 nm; finally, bulk properties of metal, like the melting temperature, are not even reached below 10 nm [37]. In this respect, depend-

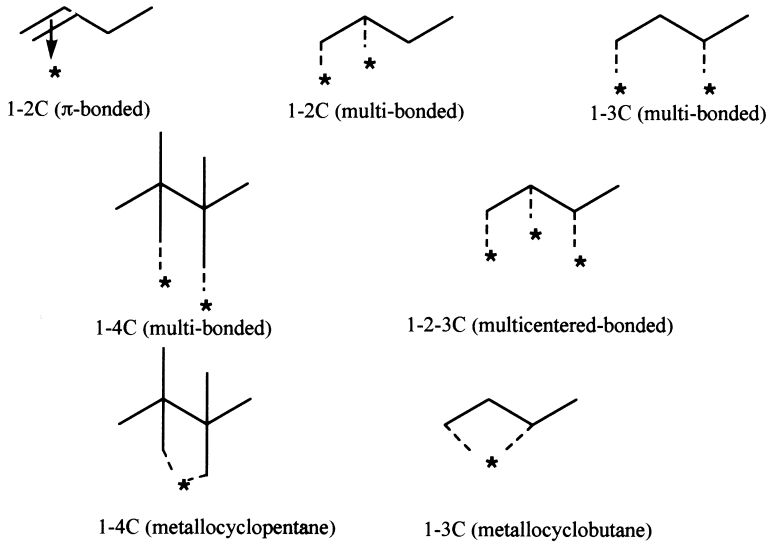

Scheme 1. Some possible adsorbed species in the case of substituted butanes.

ing on whether the reaction is more or less affected by electronic or geometric parameters, the zone where the particle size effect occurs will be different.

A second point of uppermost importance when studying intrinsic particle-size effects is to choose, as much as possible, a neutral non-active support and to avoid using conditions that could possibly induce any metal–support interaction. The procedure described above from organometallic precursors falls in this category (Section 3.1).

To illustrate these aspects, the conversion of selected alkanes over a series of Rh/Al_2O_3 is presented [20,28]. The catalysts were prepared from Rh acetylacetonate and γ-Al_2O_3 ($S_{BET} = 200\ m^2\ g^{-1}$, chlorine free). By varying the amount of Rh and the nature of the activation treatment, Rh particles with mean particle size from 13 nm to less than 1 nm have been obtained; this corresponds to a fraction of metal exposed of between ca. 0.07 and 1. The reactions of *n*-hexane (nH), 2,2,3,3-tetramethylbutane (TeMB) and methylcyclopentane (MCP) with hydrogen were carried out at atmospheric pressure in a microflow reactor. The conversion was kept low to avoid secondary reactions and mass transfer limitations. Tables 1 –3 present the data obtained from the catalytic tests.

Interesting features can be seen in the conversion of alkanes over Rh catalysts. The first one is that skeletal rearrangement remained quite marginal, usually less than 5%, whatever the Rh dispersion; the main products came from hydrogenolysis. The inability of Rh to promote isomerization may be understood in terms of metallocarbene chemistry. The metals which possess better capacities to form metallocarbenes are also the best for C–C hydrogenolysis, namely Ni > Rh > Ir > Pt [33]. In the hydrocracking of nH on large Rh particles, the main product was methane in large excess ($C_1 \gg C_5$). This behavior clearly shows that several consecutive C–C

Table 1
Catalytic properties of Rh/Al_2O_3 for the conversion of methylcyclopentane at 493 K; $P(H_2)=94$ kPa, $P(MCP)=6.2$ kPa

H/Rh[a]	d_p (nm)[b]	TOF (h^{-1})	Product distribution (mol%)					
			C_1	iC_4	iC_5	2MP[c]	3MP[c]	nH
1.5	<1	43	11.5	1.7	4.9	42.5	27.0	11.0
0.9	1.2	192	2.1	0.2	0.2	67.6	24.3	3.8
0.74	1.4	306	3.7	0.4	2.1	65.1	24.1	3.6
0.35	3.0	510	—	—	—	72.5	23.5	2.2
0.08	13	360	8.4	0.9	4.1	61.3	21.7	2.4

[a] Number of H atoms chemisorbed per Rh atom at 298 K.
[b] Mean particle size determined from transmission electron microscopy.
[c] 2MP: 2-methylpentane, 3MP: 3-methylpentane.

Table 2
Catalytic properties of Rh/Al_2O_3 for the conversion of nH at 493 K; $P(H_2)=93$ kPa, $P(nH)=6.8$ kPa

H/Rh	d_p (nm)	TOF (h^{-1})	Product distribution (mol%)				
			C_1	C_2	C_3	nC_4	nC_5
1.5	<1	185	21.8	24.8	20.6	21.8	10.8
0.9	1.2	98	16.0	25.8	25.6	23.4	9.0
0.74	1.4	116	23.0	21.0	21.0	19.6	13.4
0.35	3.0	67	21.0	19.1	23.3	18.3	18.3
0.08	13	65	43.6	11.9	14.9	13.2	16.4

Table 3
Catalytic properties of Rh/Al_2O_3 for the conversion of TeMB at 493 K; $P(H_2)=98$ kPa, $P(TeMB)=2.2$ kPa

H/Rh	d_p (nm)	TOF (h^{-1})	Product distribution (mol%)		
			C_1	iC_4	223TrMB[a]
1.5	<1	6.5	49.6	4.4	45.9
0.9	1.2	7.6	16.6	68.0	15.4
0.74	1.4	24	11.6	78.7	9.7
0.35	3.0	20	4.7	91.4	3.9
0.08	13	33	5.9	91.5	2.6

[a] 223TrMB: 2,2,3-trimethylbutane.

bond ruptures occur before desorption. Triple or multiple attachments to the surface may, therefore, be possible on Rh (multicentered-bonded species, Scheme 1), leading to complete degradation to single-carbon species, which then desorbs as methane. When the Rh particle size decreases, this behavior tends to disappear.

The second feature is the very different behavior concerning particle size sensitivity

depending on the hydrocarbon reacted: nH and MCP hydrogenolyses showed appreciable changes in TOF, but to a lesser extent in selectivities. By contrast, clear changes in both activity and selectivity occurred with TeMB hydrogenolysis. Whereas for the conversion of TeMB and MCP the TOF increases when the dispersion decreases, the reverse is observed for nH. This different behavior can hardly be interpreted by a single mechanism of C–C hydrogenolysis, and we proposed to relate it to the formation of different intermediates depending on the coordination of the surface atoms and the nature of the processed alkane [38].

In particular, the conversion of TeMB appeared to be very sensitive to the surface structure and was able to detect subtle changes in the surface topology of Rh particles. The smallest particles catalyze practically pure demethylation ($\alpha\gamma$ route), whereas large particles promote central C–C cleavage to i-butane ($\alpha\delta$ route). We proposed that the surface intermediates is a 1–3C adsorbed species on sites of low coordination (kinks, steps, edges, corners, etc.) and a 1–4C adsorbed species on sites of higher coordination (dense planes) [20,38]. In contrast, the hydrogenolysis of nH can proceed by several routes involving π-allyl, 1–2C, and 1–3C adsorbed species [38]. This is probably why it appeared much less structure sensitive. This is shown in Scheme 2, where the possible pathways for nH, MCP and TeMB hydrogenolyses are illustrated.

These results emphasize the extreme sensitivity of TeMB hydrogenolysis to the surface structure of Rh particles, which is particularly true for metal particles smaller than 2 nm. This is not specific to Rh; a similar particle size sensitivity was found for Ru [21] and for Pt [24], although it is less marked than for Rh. If particles larger than 2 nm give iC_4 selectivities higher than 90% (whatever the metal), particles smaller than 1 nm yield 50% CH_4 + TrMB for Pt at 553 K [24], 55% for Ru at 473 K [21], and 95% for Rh at 493 K (Table 3).

A better description about the nature of the 1–3C and 1–4C adsorbed species in the conversion of TeMB on Ru/Al_2O_3 was identified from kinetics [39]. Fig. 2 shows the rate dependence of the $\alpha\gamma$ and $\alpha\delta$ routes, via the 1–3C and 1–4C complexes respectively, as a function of H_2 pressure on large and small Ru particles. The kinetic analysis of these plots allowed one to derive a rate expression which showed that: (i) on small particles ($\approx$1 nm), three H atoms were abstracted from TeMB to form the 1–4C complex before C–C bond-breaking occurred, but only two H atoms were abstracted to form the 1–3C complex; (ii) on large Ru particles (4–5 nm), five H atoms were removed from TeMB to form the 1–4C complex. On the basis of a logical mechanism, Scheme 3 shows the proposed surface complexes for TeMB hydrogenolysis on Ru/Al_2O_3 catalysts [39].

The different degrees of dehydrogenation of the surface intermediates highlight the different particle-size sensitivity of the routes via the 1–3C or 1–4C complexes at the same H_2 pressure, or the H_2 pressure dependence on the same Ru/Al_2O_3. This is a typical illustration of an ensemble-size effect where the accommodation of the surface complex requires an increased number of free neighboring Ru atoms when the surface complex becomes more and more dehydrogenated. From this point of view, the involvement of geometric considerations is of a great concern. However, the bond strength of hydrogen changes slightly with particle size [40] and it could

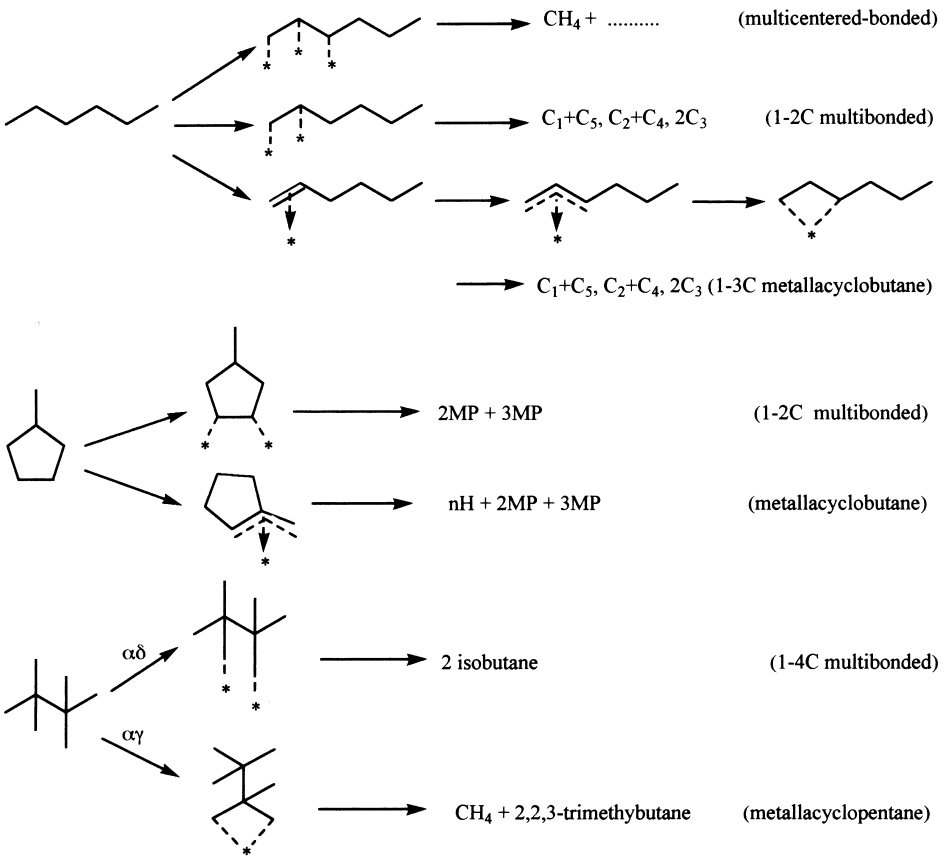

Scheme 2. Some possible routes for the conversion of nH, MCP and TeMB.

then be speculated that the easier dehydrogenation of the intermediate on large particles is related to the higher heat of adsorption of hydrogen, which displaces the equilibrium. Similar conclusions were also reached from the kinetics of TeMB hydrogenolysis on Rh/Al_2O_3 of various Rh particle sizes [40].

From these observations we suggested that TeMB hydrogenolysis can constitute a powerful chemical probe for identifying subtle changes in the topology and the coordination of the active sites in very small particles. This approach was developed, in particular, to study the ensemble-size effect in bimetallic catalysts and when metal–support interaction occurs.

4.2. Ensemble-size effects

Multimetallic formulations are currently in use to improve the properties of metal catalysts. Over recent decades the addition of Sn, Re or Ir to Pt has led to new

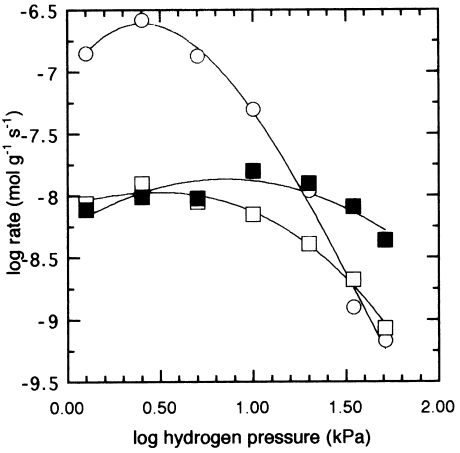

Fig. 2. Hydrogen pressure dependence for the rate of αγ (full symbols) and αδ (open symbols) routes in TeMB hydrogenolysis at 463 K on Ru/Al_2O_3 of large particles (○, $d_p = 4$ nm) and small particles (□,■, $d_p = 1$ nm).

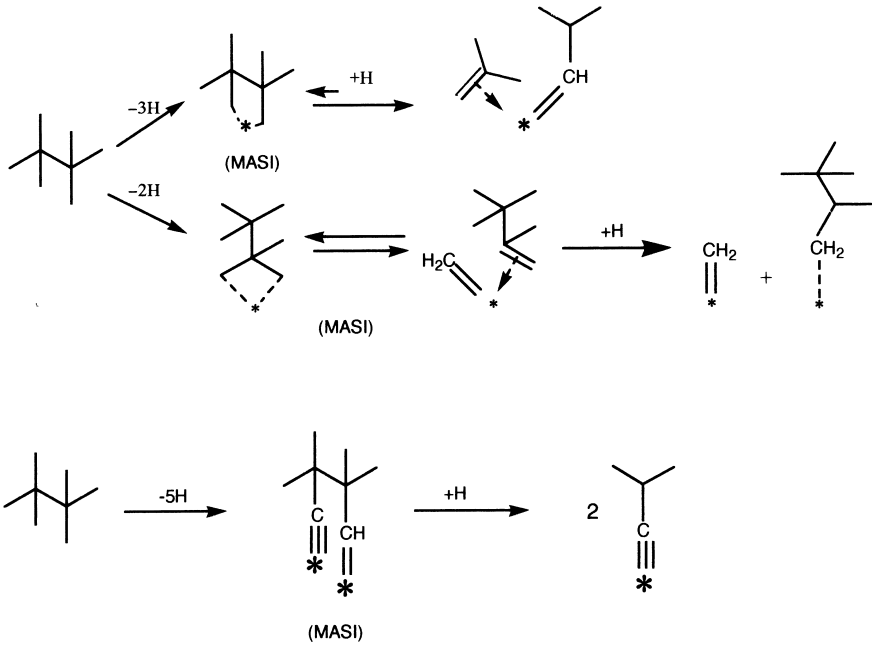

Scheme 3. αγ and αδ routes in the hydrogenolysis of TeMB on large and small Ru particles. MASI: most abundant surface species; the size of the asterisk is indicative of the ensemble size.

generations of reforming catalysts with better selectivity for isomerization and aromatization, and longer lifetime on stream [41].

For both technical and academic reasons, the way by which the second component modifies the properties of pure metals is a subject of interest and is still not well elucidated. Depending on the reaction and the operating conditions considered, geometric and/or electronic effects were claimed (see Refs. [6,41] for a review). In any event, understanding of the bimetallic effect would require the best possible knowledge of the following points: (i) are the two elements intimately interacting in the same aggregates? (ii) does surface segregation of one component occur? (iii) are the two elements randomly distributed in the surface layer or not?

The first point is not totally fulfilled when preparing bimetallic catalysts by classical means. By contrast, the controlled surface reaction method (Section 3.2) allows one to prepare some bimetallic catalysts in which the two components are in much closer interaction.

The second question to be asked is the surface composition in bimetallic particles. The occurrence of segregation of one component of an alloy to the surface is now well established, as well as its influence on the catalytic properties (see Refs. [6,41]).

On small particles (1–2 nm) surface atoms tend to represent the majority of the atoms of the particle and the surface enrichment loses meaning. Nevertheless, on these small aggregates the surface contains sites of different topologies: low-index planes, kinks, edges, corners, etc. The distribution of the different components of the bimetallic particles could be ordered, i.e one component would occupy sites of a given topology preferentially, or could be disordered [42–44]. Unfortunately, experimental evidence for this phenomenon is lacking, and, so far, spectroscopic techniques like EXAFS do not appear accurate enough to validate these concepts. In this regard, the conversion of TeMB, which is highly sensitive to changes of surface topology, can solve this problem.

We have thus studied the kinetics of TeMB hydrogenolysis on a series of Ru/Al_2O_3 modified by Sn or Ge [39]. The bimetallic catalysts were prepared from the same parent Ru/Al_2O_3 (1%Ru, H/Ru = 0.9, $d_p \approx 1$ nm) and $Sn(C_4H_9)_4$ or $Ge(C_4H_9)_4$ to give $RuSn/Al_2O_3$ (0.26%Sn, H/Ru = 0.51, $d_p \approx 1$ nm) and $RuGe/Al_2O_3$ (0.70%Ge, H/Ru = 0.41, $d_p \approx 1$ nm). Fig. 3 shows the rate dependence as a function of H_2 pressure for the $\alpha\gamma$ (1–3C) and $\alpha\delta$ (1–4C) routes in TeMB hydrogenolysis on these catalysts. Whereas the selectivity changes significantly with alloying, the TOF was only marginally affected. This is because the addition of Sn did not change the specific activity and the addition of Ge decreased it by a factor of 2–3 only. The effect was stronger on the $\alpha\delta$ route when Ge was added, but the reverse was true for Sn. This situation, in which activity changes so little while selectivity is greatly affected, can hardly be attributed to any electronic modification of the surface. This is a reflection of (i) the occurrence of $\alpha\gamma$ and $\alpha\delta$ routes on specific sites and (ii) different locations for Ge and Sn atoms on the surface.

We have concluded that the $\alpha\delta$ process occurs on the sites of highest coordination of a given particle (dense plane), whereas the $\alpha\gamma$ process takes place on low coordination sites (kinks, edges, corners, etc.). As a result, the preferential location of Sn at defect sites, corners and edges in RuSn aggregates was postulated. The same

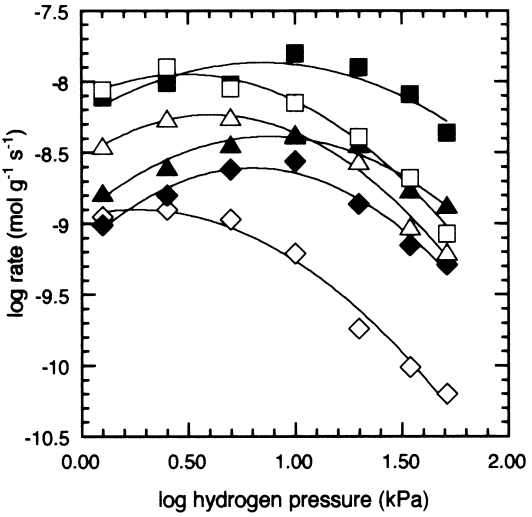

Fig. 3. Hydrogen pressure dependence for the rate of αγ (full symbols) and αδ (open symbols) routes in TeMB hydrogeolysis at 463 K on small metallic particles of Ru/Al_2O_3 (□,■), $RuSn/Al_2O_3$ (▲,△) and $RuGe/Al_2O_3$ (◇,◆).

approach, developed for RuGe aggregates, has shown that Ge does not have such a definite site preference and is distributed in a more random fashion in the surface layer. This behavior seems confirmed by EXAFS experiments [45] and quantum chemical calculations on bimetallic model clusters [46,47]. EXAFS of Ru/Al_2O_3, $RuSn/Al_2O_3$ and $RuGe/Al_2O_3$ showed that Ge is more diluted in the Ru matrix than Sn [45]. From quantum chemical calculations on Ru_9, Ru_8Ge and Ru_8Sn clusters using the functional density method, we concluded that Sn and, to a much smaller extent, Ge prefer to be localized at the sites of lower coordination [46]. Similar calculations on Ru_{13}, $Ru_{10}Ge_3$ and $Ru_{10}Sn_3$ clusters with perfect cubo-octahedral shape emphasized that Ge–Ge bonds are less favored than Sn–Sn bonds at the surface of these aggregates, all surface atoms having the same coordination number of 5 [47].

A quantum chemical study and kinetic experiments on alkane hydrogenolysis have shown that in small RhM/Al_2O_3 (M = Sn, Ge, Pb) catalysts, Pb and Sn are preferentially located in that case at low coordination sites of the bimetallic aggregates, whereas Ge is more randomly distributed too [28]. Similar conclusions were reached from the chemisorption of CO on RhM/Al_2O_3 [48] and PtM/Al_2O_3 [49] (M = Sn, Pb) catalysts, and from kinetic experiments alone in the RhPd [50], RhCu [51], RuCu [52] and PtSn [24] systems where Pd, Cu and Sn should occupy the low coordination sites.

The topology and the environment of the active centers can also be altered by cyclic oxido-reduction thermal treatments and by the extent of metal–support interactions. The so-called strong metal–support interaction (SMSI) refers to the peculiar interaction occurring between small particles and a reducible carrier, like TiO_2. A

strong decrease of H_2 chemisorption is the fingerprint of this phenomenon, first described by Tauster and Fung [53] in the case of Pt/TiO_2 reduced at 773 K. The SMSI effect was recently reviewed by Haller and Resasco [7]. Two explanations were proposed for SMSI: (i) the first argues that a modification of the metal d-band occurs from interaction with partially reduced Ti^{3+}; (ii) the second proposal assumes a migration of partially reduced TiO_x species onto the surface of the metallic particles. Geometric considerations underlie the second proposal and C–C hydrogenolysis could be a sensitive probe of its occurrence, in particular TeMB hydrogenolysis.

TeMB hydrogenolysis carried out on titania-supported Ru [54] and Rh [20] catalysts reduced at various temperatures provided evidence that the $\alpha\gamma$ route was favored when the catalysts entered the SMSI state, i.e. when reduced at high temperature. This behavior parallels that of adding Ge to Ru or Rh and agrees with a decoration of the metallic particles with TiO_x patches, and distributed in a random fashion. However, the near constancy of TOF in an SMSI state shows that electronic effects intervene also, probably by a modification of the heat of H_2 chemisorption.

Similar conclusions about some mixing between geometric and electronic considerations were suggested when an Ru/Al_2O_3 was submitted to cycling oxido-reduction treatments [55]. After reduction of a parent Ru/Al_2O_3 (1% Ru, $H/Ru = 0.9$) at 623 K, then oxidation at 623 K and reduction again at 433 K, there is a great decrease of H_2 uptake ($H/Ru = 0.15$) and the individual particles are aggregated in "corrugated" flat, highly disordered, particles. These particles exhibited an extremely high reactivity for ethane, propane, *n*-butane and TeMB hydrogenolyses, which was suppressed after annealing back the catalyst at 753 K, but not the H_2 uptake which remained the same. This structural effect, previously described by Gao and Schmidt for Rh catalysts [56], still remains a little puzzling. Possible explanations in terms of either surface morphology or of alterations in electronic character were considered [55]. Significant changes in the adsorption constants of the alkanes and H_2 were indeed identified.

These studies on the hydrogenolysis of C–C bonds in alkanes have taught us that:

(1) the structure sensitivity of the C–C bond cleavage depends on the alkane considered, the nature of the metal and the reaction conditions;
(2) the differences in structure sensitivity come from the occurrence of a wide variety of surface complexes which operate depending on the nature of both the alkane and the metal particles;
(3) the examination of the changes of selectivity in the conversion of a chosen alkane is richer in information than considering TOFs;
(4) besides an interest in better knowledge of the parameters affecting C–C bond cleavage, the use of selected reactions is a very powerful probe for identifying subtle changes in surface topology. In particular, TeMB hydrogenolysis provides good insight on the structure of metallic particles in the 1 nm region, where physical methods could be limited.

5. Hydrogenolysis of carbon–halogen bonds

Halogen-containing organic compounds, especially those containing chlorine, are noxious for the environment. Polychlorinated aromatics and chlorofluorocarbons

(CFCs) are particularly charged with these problems. Polyaromatic wastes participate in the contamination of soils and water, and CFCs are responsible for the seasonal depletion of the ozone layer in the stratosphere and for the greenhouse effect [57]. The present available destruction technologies are: (i) combustion at high temperatures (>1000 °C), with the potential risk of the formation of highly toxic compounds like dioxins; (ii) catalytic combustion at medium temperatures (300–500 °C); (iii) hydrodehalogenation at low temperatures (<300 °C). This latter process is a particularly elegant solution proposed for the transformation of banked CFCs (≈2 million tons worldwide) into valuable substitutes, i.e. the hydrofluorocarbons (HFCs).

The problems raised by the destruction of CFCs and the synthesis of their substitutes have recently been reviewed by Wiersma et al. [58] and Manzer and Mallikarjuna Rao [59]. Companies, like Dupont, ICI and Elf Atochem, which have a great concern with these compounds, have claimed several processes for the production of HFCs from CFCs (see Refs. [58,59]). Although this topic was often claimed for challenging researches in the field of catalysis by metals [60,61], it has only raised few fundamental studies on the kinetics and mechanism of the reaction [62–68]. Hereafter, an overview on some conclusions we reached on the mechanism of C–halogen bond cleavage, and its structure-sensitivity, is presented.

5.1. Kinetics and mechanism of the C–halogen bond hydrogenolysis

We have studied the kinetics of C–halogen bond scission on supported Pd and Rh catalysts in both aromatic and aliphatic series. In the aromatic series, chlorobenzene (CBz) was chosen as a model molecule and the reaction was carried out between 320 and 370 K in the gas phase using a fixed bed reactor [69]. The catalysts were alumina-supported Pd and Rh with H/metal ratios (fraction exposed) ranging from 0.03 to 1. The reaction of CBz with H_2 yielded benzene and HCl. Kinetics data showed that (i) hydrogen reacts in the dissociated form in the rate-determining step and (ii) CBz and HCl compete and interact strongly with the surface. Harper and Kemball [70] have shown that the interaction of fluorobenzene and a metal surface corresponds to a fluorination. Moreover, Boyes et al. [67] have shown from XPS studies that the active Pd state during the hydroconversion of CF_3CFCl_2 was a surface Pd "chloride". We have thus proposed that a chlorination–dechlorination process of the Pd or Rh surface could explain the conversion of CBz with H_2. This reaction is formally identical to the mechanism proposed by Mars and van Krevelen [71] for the selective oxidation of hydrocarbons and can be written as

$$\text{Pd–H} + \text{C}_6\text{H}_5\text{Cl} \xrightarrow{k_1} \text{Pd–Cl} + \text{C}_6\text{H}_6 \quad (1)$$

$$\text{Pd–H} + \text{Cl} \xrightarrow{k_2} \text{Pd–Cl} + \text{H}_2 \quad (2)$$

$$\text{Pd–Cl} + \text{H}_2 \xrightarrow{k_\text{H}} \text{Pd–H} + \text{HCl} \quad (3)$$

The reaction in Eq. (1) probably implies the dissociative adsorption of CBz, which can also be described as an oxidative addition on the Pd atom, followed by the elimination of benzene. The surface is reduced by H_2 in the step shown in Eq. (3), and the competition between HCl and CBz is readily explained. The rate equation can be obtained by assuming that at the steady state the rates of reduction and chlorination of the surface are equal, which gives

$$r = \frac{k_1 k_H P_{CBz} P_{H_2}^{0.5}}{k_1 P_{CBz} + k_2 P_{HCl} + k_H P_{H_2}^{0.5}} \quad (4)$$

The rate constants k_H, k_1 and k_2 were obtained by fitting Eq. (4) to the kinetic data for the different catalysts. The correlation coefficient was generally higher than 0.97. The dependence of these rate constants on temperature was estimated for $PdSn/Al_2O_3$ bimetallic catalysts [72]. It appeared that the reduction of the "chlorinated" surface is a much more activated process than chlorination of the reduced surface, which is practically not activated; chlorination by CBz exhibits an intermediate behavior. We have, however, to keep in mind that within the restricted pressure ranges investigated ($2 < P(H_2) < 100$ kPa, $0.15 < P(CBz) < 10$ kPa), other kinetic laws could be fitted with some satisfaction. This is, in particular, the case of Langmuir–Hinshelwood kinetics which was suggested to apply in the hydroconversion of substituted benzenes [73] and polychlorobiphenyls [74].

In the aliphatic series, the kinetics of CF_2Cl_2 hydrodehalogenation was studied between 420 and 520 K in the gas phase using a fixed bed reactor. The catalysts consisted of Pd supported on AlF_3 and graphite [63]. The kinetic data were fitted to a Langmuir–Hinshelwood model and the halogenation–dehalogenation mechanism described above (Eq. (4)). It appeared that very little difference existed between the models, in the range of reactant pressure investigated ($0.1 < P(CF_2Cl_2)/P(H_2) < 3$). One can, moreover, point out that the kinetic data reported for the hydrodehalogenation of CF_3CFCl_2 on Pd/Al_2O_3 [65] are in good agreement with this model. Two differences appeared for the relative interaction between the Pd surface with H_2 and either CBz or CF_2Cl_2. The interaction is much stronger, as well as the inhibiting effect of CBz, in the case of CBz. Moreover, the inhibiting effect of HCl released during the hydrodehalogenation of CF_3CFCl_2 on a polycrystalline Pd foil was proved from kinetics [75].

Some aspects of the mechanism of the CF_2Cl_2 conversion appeared quite interesting. This CF_2Cl_2 transformation can be formally written as

$$CF_2Cl_2 \xrightarrow{H_2} CH_2F_2 \xrightarrow{H_2} CH_4$$

For normal serial reactions the selectivity to the end product, methane, should be nil at zero conversion and should increase with decreasing space velocity. Actually, this was not observed since the initial CH_4 selectivity was about 10–20%, depending on the catalyst, and only smoothly increased with conversion [63,64]. Moreover, the reactivity of the postulated intermediates, $CHFCl_2$, CH_2F_2 and CH_3F, was very low compared with that of CF_2Cl_2. A simplified rake scheme mechanism (Scheme 4)

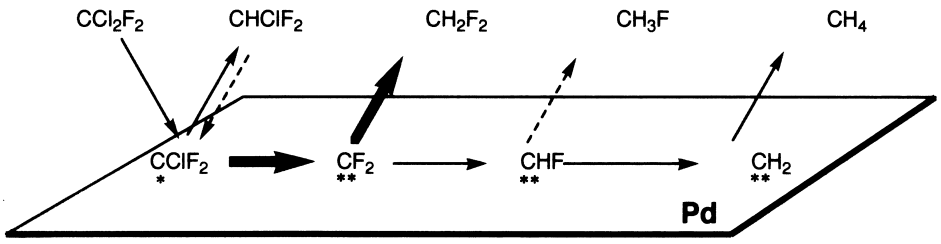

Scheme 4. Proposed reaction mechanism for the hydrodehalogenation of CF_2Cl_2.

was thus postulated [63,64]. This rake scheme is very similar to that proposed by Germain [76] to apply in the selective oxidation of hydrocarbons.

In the hydrogenation of CF_2Cl_2, the most abundant surface intermediate would be the adsorbed $*CF_2$ species. The selectivity for the main products, CH_2F_2 and CH_4, is mainly determined by the ratio between the desorption rate of $*CF_2$ assisted by hydrogen to give CH_2F_2 and the rate of the surface reaction leading to CH_4. A similar rake scheme applies for the conversion of CF_3CFCl_2 on Pd-based catalysts, which yielded CF_3CH_2F and CF_3CH_3 as primary products [62,65,67,75]. The uppermost importance of palladocarbenes in the conversion of CFCs has thus been emphasized. On the other hand, the hydroconversion of CCl_4 over supported Pt catalyst leads to $CHCl_3$ and CH_4 as primary products too [77,78].

5.2. *Particle-size effects*

Very few studies have dealt with the structure-sensitivity of the C–halogen hydrogenolysis. In the conversion of CBz [69], as in that of CF_2Cl_2 [63], the rate constants for the dehalogenation and for the regeneration steps, determined from Eq. (4), decreased with the size of metal particles. This decrease of the rate constants, by a factor of 10–100, was ascribed to modifications in the electronic properties of Pd [69]. The final result of this structure sensitivity is higher values of TOF for large Pd particles [69]. Similar phenomena were reported for the conversion of CF_2Cl_2 and CF_3CFCl_2 [65]. Those authors proposed electronic and geometric considerations for this behavior: the dense planes present on large Pd particles will be the active and selective sites for hydrodechlorination. The orientation of the reaction of CF_2Cl_2 to CH_2F_2 or CH_4 is also modified by the size of the Pd particles; Pd particles larger than 8 nm provide more than 80% CH_2F_2 selectivity [63,66].

5.3. *Metal–support interaction*

The comparative behavior of Pd/graphite (CH_2F_2 selectivity $\approx 60\%$) and of Pd/AlF_3 (CH_2F_2 selectivity $\approx 80\%$) suggested the occurrence of some kind of metal–support interaction in the reaction [63]. In the preparation of Pd/AlF_3 catalysts, hydrogen fluoride was released during the final step of reduction. We could speculate that AlF_x species ($_x < 3$) were formed at the periphery and on the Pd particles. In

the course of CF_2Cl_2 hydrogenation, these species would withdraw adsorbed fluorine atoms, hence scavenging the surface and protecting the Pd particles against the diffusion of fluorine into the bulk. Indeed, we proposed for Pd black and Pd/graphite that fluorine atoms occluded into Pd would be responsible for the lack of selectivity to CH_2F_2 [63]. However, Wiersma et al. [64] found that Pd/carbon catalysts did not exhibit poor selectivity to CH_2F_2, but the reaction was carried out with a much higher H_2 partial pressure.

Finally, one should remark that if Pd/Al_2O_3 was not selective when the reaction was started, it became as selective as Pd/AlF_3 as the reaction proceeded thanks to the partial fluorination of alumina to fluoride and oxifluoride species [63,79]. Table 4 shows that amorphous Al_2O_3 and TiO_2, which were transformed into "AlF_3"- and "TiF_3"-like supports by attack with the released HF, were selective supports. In contrast, crystalline ZrO_2, which could not be fluorinated into "ZrF_4", did not exhibit high CH_2F_2 selectivity [79]. The importance of AlF_x adspecies on Pd particles was emphasized by the behavior of Pd/graphite catalyst promoted with Al, by reacting a Pd/graphite with $Al(C_2H_5)_3$ in H_2. Al species deposited onto Pd transform to AlF_x in the course of the reaction and the catalyst Pd"Al"/graphite became selective [79].

The influence of the nature of both the supports and the metallic precursors was also proved in the hydrodechlorination of CCl_4 on Pt-based catalysts [77,80,81]. The fate of the adsorbed $*CCl_3$ species, either to be hydrogenated to $CHCl_3$ or to suffer H/Cl exchanges in the adsorbed state, is the key point which determines the selectivity to $CHCl_3$ or CH_4.

6. Hydrogenation of halonitrobenzenes and of α,β-unsaturated aldehydes

The sensitivity of C–C bond rupture and C=C bond hydrogenation to the structure has been convincingly demonstrated in the reaction of short hydrocarbons [4], and has been the subject of much basic research. This is not the case for the

Table 4
Distribution of the products for the hydrogenation of CF_2Cl_2 at 453 K over Pd-based catalysts ($CF_2Cl_2/H_2 \approx 0.3$–0.35 mol/mol, conversion $<10\%$)

Catalyst	$(H/Pd)_{irr}$	Product selectivity (mol%)			
		CH_4	CH_2F_2	CHF_2Cl	Others[a]
Pd/graphite	0.15	40.5	56.1	1.7	1.7
Pd/Al_2O_3	0.12	16.5	79.1	3.2	1.0
Pd/AlF_3	0.10	13.9	80.3	1.7	4.0
Pd/TiO_2	0.08	12.0	83.6	4.3	0.1
Pd/TiF_3	0.23	13.1	81.8	4.9	0.2
Pd/ZrO_2	0.33	48.9	31.4	8.7	10.8
Pd/ZrF_4	0.05	9.6	86.0	3.8	0.1

[a] $CH_3F + CHFCl_2 + CF_3Cl$.

hydrogenation of organic compounds containing unsaturated groups like $-NO_2$, –NO, keto, nitrile, etc. The reasons for this lack of study are readily understandable: the worldwide market for catalysts in 1993 was estimated to be US$4589 million and the amount for catalysts used in organic synthesis was US$1753 million. Within this latter group, the hydrogenation catalysts represent US$174 million and are extremely disseminated in a very wide variety of reactions. By contrast, the reforming catalyst alone represents a market of US$95 million. The economic stakes for the optimization of the reforming catalysts (Pt+Sn, Ir, Re, etc.) were thus noticeably different from those for the hydrogenation catalysts in fine chemical synthesis. For these latter processes, rather than focusing on the development of intrinsically selective catalysts, the approach has been to modify the reaction media by the addition of selectivity promoters, like bases, acids or metal salts. An archetypal and historical example is the selective hydrogenation of α,β-unsaturated carbonyls, which dates back to 1925. Tuley and Adams [82] used unsupported Pt catalysts promoted by Zn and Fe chlorides for the liquid-phase hydrogenation of cinnamaldehyde (CAL) to cinnamyl alcohol (COL). However, such processes generated large amounts of by-products, and needed separation steps to recover the target compound. This is a key aspect for many hydrogenations widely employed in fine chemistry, and a field of challenging research to develop intrinsically chemico-, regio- and enantio-selective hydrogenation catalysts by tuning the particle morphology and metal–support interaction, and by the development of multimetallic formulations. This tendency is observed in the books of proceedings on the "Conference on Catalysis of Organic Reactions" and "Heterogeneous Catalysis and Fine Chemicals" (see Refs. [83,84] for the last in these series).

Compared with the hydrocarbons processed in the refining industry, the substrates of fine chemistry are, on average, of higher molar weight and contain functional groups which interact strongly, e.g. by hydrogen bonding. Thus many of them are liquids or solids and their hydrogenations must therefore be conducted in the liquid phase or in solution. This simple fact creates numerous problems for the scientist wishing to conduct fundamental research, and the structure-sensitivity is more difficult to prove unequivocally. This could be due to (i) the solvent effect and (ii) limitation in the diffusion of reactants through the liquid to the surface of the catalyst. As a result, the sensitivity to the structure is better proved on the basis of selectivity patterns than on TOFs. This is the case when a substrate contains two functional groups of comparable reactivity: these may be either (i) two unsaturated groups, or (ii) one unsaturated group and another susceptible to hydrogenolysis. These may be illustrated by two of the classic problems of catalytic hydrogenation of unsaturated aldehydes and of substituted nitrobenzenes. As in many other transformations in organic synthesis, these hydrogenations run through a sequence of consecutive and parallel elementary reactions. This is illustrated for the hydrogenation of CAL (Scheme 5). In this formal reaction scheme, the selectivity to COL, the target compound, is determined by (i) the initial attack of CAL on the C=C or C=O double bonds, which depends on both geometric and electronic factors, and (ii) the desorption of COL or its further hydrogenation to hydrocinnamyl alcohol (HCOL), which is mainly affected by electronic factors. This will be illustrated by

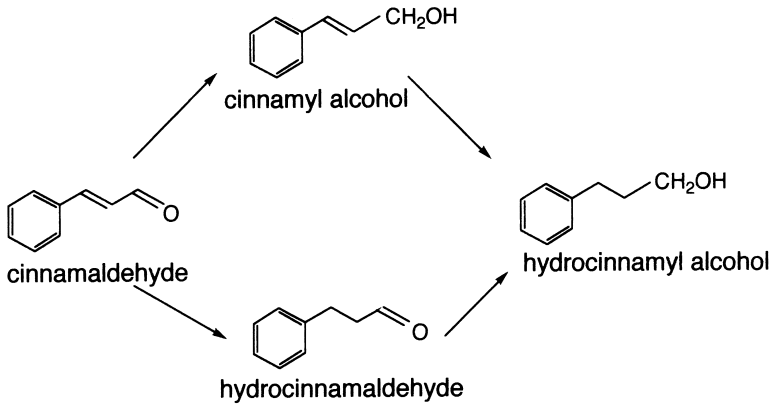

Scheme 5. Formal reaction scheme for the hydrogenation of CAL.

the effect of particle size, bimetallic and metal–support interaction on the above-mentioned reactions.

6.1. *Particle-size effect*

6.1.1. *Hydrogenation of* p-*chloronitrobenzene (CNB)*

The selective hydrogenation of halonitroaromatics is an old problem, still attractive, for the production of substituted anilines. The aromatic ring activates the C–halogen bond, rendering it easy to hydrogenate, so that it is difficult to avoid the formation of some aniline (Scheme 6). Losses of selectivity also originate in the formation of bimolecular intermediates (azoxy, azo, hydrazo), which should, however, ultimately yield the substituted anilines. Pt-based catalysts are the best for this reaction for minimizing dehalogenation combined with a fast rate of nitro-group reduction [85]. However, the selectivity of Pt needs to be improved by the addition of promoters, usually in the reaction medium.

The linear decrease of the rate of nitrobenzene hydrogenation as a function of Cu coverage of Pt black, coated with Cu, suggested that the reduction of the nitro-group proceeds on a surface site formed by a single Pt atom [86]. However, the TOF of nitrobenzene hydrogenation decreased when the size of supported Pd particles decreased [87]. From these observations we could thus conclude that the structure sensitivity of this reaction is dominated by electronic factors.

We have thus studied the liquid-phase hydrogenation of CNB in a batch reactor,

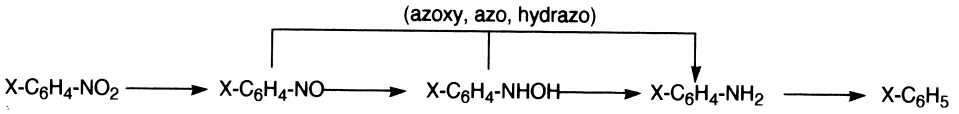

Scheme 6. Formal reaction scheme for the hydrogenation of halonitrobenzenes.

Table 5
Characteristics of the kinetics of hydrogenation of CNB over Pt/Al_2O_3 catalysts (at 60% CNB conversion)

H/Pt	d_p (nm)	Rate constant (mol s^{-1} g^{-1}) $\times 10^6$	Specific rate constant per Pt_s atom (s^{-1})	$\lambda_{CNB}/(\lambda_H P_H)^{0.5}$ (dm^3 mol^{-1})	Selectivity to CAN (mol%)
0.09	12.0	≈170	≈17	≈0.9	96.4
0.26	3.4	290	10.5	0.91	82.4
0.4	2.3	60	6.1	3.5	83.9
0.99	1.2	190	2.65	4.95	82.1

at low temperature (303 K) and atmospheric pressure, in methanol as solvent. The catalytic properties were characterized by the initial rate of reaction, expressed as TOF, and the yield or the selectivity in chloroaniline (CAN). The kinetic law was derived from the initial rate, since the low concentration of products then simplifies the kinetics. The kinetic effect of the products was determined accurately by adding them in the initial reaction mixture and measuring back the initial rate.

On both Pt [88] and Ru [89] catalysts the initial rate went through a maximum value as a function of CNB concentration, in the range of the concentration and pressure of reactants used. This behavior reflects the competitive adsorption between hydrogen and CNB for the same Pt sites. However, the rate did not fall to zero at high CNB concentration, as expected for a classical Langmuir–Hinshelwood kinetic model with competitive adsorption of the reactants. Actually, the rate tended to an asymptotic value. In order to rationalize this peculiar behavior, a modified Langmuir–Hinshelwood kinetic model was proposed based on the following assumptions:

(1) a competitive adsorption between H_2 and CNB occurring at low or medium concentrations;
(2) at high CNB concentrations, the Pt surface is saturated with respect to CNB adsorption, thus suggesting a strong interaction between nitrobenzene and the surface. The fact that nitrobenzene cannot completely expel hydrogen from the surface may be due to dipolar interactions and/or steric hindrance. In that case the substrate cannot cover all the Pt surface and a fraction of sites is still available for the chemisorption and the dissociation of the much smaller hydrogen molecule. The detailed kinetic analysis [88] showed that this fraction of Pt sites remaining free for H_2 adsorption at saturation of the surface by CNB was low and ranged between 0.07 and 0.16.

The kinetic analysis of the behavior of a series of Pt/Al_2O_3 catalysts (Table 5) of varying dispersion ($0.09 < H/Pt < 1$; $12 > d_p > 1$ nm) resulted in evidence that [88]:

(1) the relative adsorption strength between CNB and H_2 (λ_{CNB}/λ_H) tends to increase slightly on small particles;
(2) when expressing the rate constant K of the surface reaction (hydrogen addition on the CNB* adsorbed species) on a per site basis (TOF) the effect of metal particle size appears rather small: the change of TOF as a function of Pt dispersion did not exceed one order of magnitude. This effect of particle size

Table 6
Inihibitor effect of *p*-chloraniline on the initial rate of CNB hydrogenation on Pt catalysts at 303 K; $C_{CNB} = 0.13$ mol dm^{-3}

Sample	H/Pt	d_p (nm)	Initial reaction rate (mol s^{-1} g^{-1}) $\times 10^6$	
			$C_{CAN} = 0$	$C_{CAN} = 1.3$ mol dm^{-3}
Pt/Al_2O_3	0.09	12.0	10.8	2
Pt/Al_2O_3	1.0	1.1	18.8	0.7
$PtZn/Al_2O_3$	0.62	1.3	13	3.9
Pt/TiO_2(HT)	0.04	3.5	3.3	0.33

compares reasonably well with that reported by Carturan et al. [87] for Pd catalysts: a 30-fold increase of TOF when Pd dispersion decreases.

This behavior was interpreted as follows.

(1) When the size of metal particles decreases, the local density of states (LDS) at the Fermi level also decreases [90], which induces a higher interaction of Pt particles with CNB, compared with hydrogen, through the donor nitro-group of CNB.

(2) The value of the TOF of the surface reaction increases slightly with particle size, i.e. with the LDS at the Fermi level, which suggests that a negatively charged transition state would be expected with Pt catalysts. Such a surface species could result of the attack of N=O bonds by a weak nucleophilic agent, such as chemisorbed hydrogen, as suggested by Galvagno et al. [91]. The extent of negative charge was investigated using the Hammett relationship and substituted nitrobenzenes, and was found low [88].

The product selectivities of the CNB hydrogenation at 60% conversion are reported in Table 5. The data show that for Pt/Al_2O_3 catalysts with particles size lower than 3 nm the hydrodechlorination of CAN to aniline became significant (>15%), whereas it remained low on large Pt particles. Two explanations were proposed:

(1) the relative strength of adsorption between CNB and CAN increases when Pt dispersion decreases. Hence, CAN is easily desorbed from the Pt surface and dechlorination is suppressed;
(2) large Pt particles exhibit a lower activity for C–Cl bond hydrogenolysis than the smaller ones.

Studies on the reactivity of C–Cl bond hydrogenolysis in an aromatic series as a function of Pt particle size are scarce. However, the cleavage of that bond in CBz was found to be faster on large Pd and Rh particles supported on alumina [69]. We can then reasonably assume that a similar behavior occurs with Pt/Al_2O_3 catalysts. The first proposition above is then more likely, and agrees with the lower inhibiting effect of CAN on the initial reaction rate of CNB hydrogenation over large Pt particles (Table 6).

These results suggested that modifications in electronic properties of Pt particles

determine the selectivity. However, steric effects could also influence the selectivity, as proposed in the 2,4-dinitrotoluene hydrogenation on Pd/C catalysts [92].

6.1.2. Hydrogenation of α,β-unsaturated aldehydes

Another of these long-standing problems concerns the hydrogenation of α,β-unsaturated carbonyls, as acrolein (propenal) or CAL (3-phenylpropenal, see Scheme 5). In these cases the desired products are the unsaturated alcohols and not the saturated aldehydes or the saturated alcohols. It is well established that over Group VIII the C=C bond is hydrogenated faster than the C=O bond, and much effort has gone into finding catalysts that will achieve the desired goals. The research in this field has recently been reviewed by Gallezot et al. [93], with special emphasis on the hydrogenation of CAL. From the literature review it is evident that the selectivity to COL is better: (i) over Ir than Ru, Pt, Rh or Pd; (ii) on large metal particles; (iii) when graphite or TiO_2 are used as supports in place of carbon or silica; (iv) on metals supported on zeolites containing alkali cations; (v) on bimetallic catalysts like PtFe/C. Moreover, the selectivity depends on the substitution on the C=C and C=O bonds.

On the series of model Ru/Al_2O_3 catalysts ($0.07 < H/Ru < 0.72$; $13 > d_p > 1.3$ nm), we have studied the structure-sensitivity of (i) the gas-phase hydrogenation of acrolein [94] and (ii) the liquid-phase hydrogenation of CAL [95]. Fig. 4 shows the dependence of TOF, and selectivity to the unsaturated alcohol as a function of Ru dispersion (H/Ru), in these two reactions.

In the two reactions the TOF decreased when the Ru particle size decreased. This structure-sensitivity was not reported for the liquid-phase hydrogenation of CAL [96] and citral [97] on a series of Ru/C catalysts. However, in the latter cases the

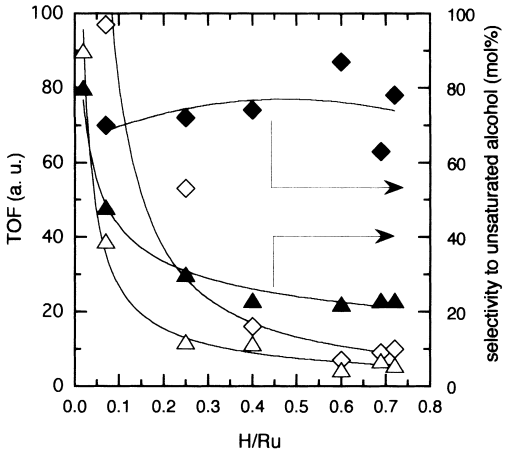

Fig. 4. TOF (open symbols) and selectivity to unsaturated alcohol (full symbols) at initial conversion in the gas-phase hydrogenation of acrolein (◇,◆) and the liquid-phase hydrogenation of CAL (△,▲) on Ru/Al_2O_3 catalysts. Conditions: P(acrolein) = 11 kPa, $P(H_2)$ = 9 kPa, $P(N_2)$ = 81 kPa, T_R = 363 K; $C_{CAL} = 7.9 \times 10^{-4}$ mol cm^{-3}, $P(H_2)$ = 4.5 MPa, T_R = 383 K, isopropanol solvent.

reaction was carried out at atmospheric pressure, and a different kinetic dependence vs. H_2 pressure as a function of Ru particle size might exist.

More interesting is the evolution of selectivity pattern with the size of Ru particles. The COL selectivity increased from 22% for an Ru particle size of ca. 1.2 nm to 80% on large crystallites of bulk Ru, in full agreement with the previous report from Galvagno et al. [96]. This effect was particularly pronounced when the Ru particles are larger than 3 nm. Interestingly, we did not observe this behavior for acrolein hydrogenation and the selectivity to allyl alcohol changed much less with Ru particle size. It is generally considered that particles larger than 4 nm suffer little change of morphology and are mainly populated with low index planes. The behavior of large particles can thus be well explained on the basis of the geometric orientation of CAL on the metal surface, as proposed by Gallezot et al. [93]. On the flat metal surface of large particles, CAL will be tilted far from the surface owing to repulsive interaction between the phenyl ring and Ru surface, thus protecting the C=C bond. By contrast, the unhindered acrolein molecule can adsorb as a flat species independent of the morphology of the Ru particles and thus showed only small changes in allyl alcohol selectivity.

On the basis of these arguments, the selectivity to the unsaturated alcohol should increase with substitution of the C=C bond, when the hydrogenation is carried out on the same Ru/Al_2O_3 catalyst. This was indeed found for the gas-phase hydrogenation of substituted acrolein. At low reactant partial pressure, $P(H_2)/P(\text{substrate}) = 7$–8, the relative rates for hydrogenation of C=O vs. C=C bonds was 0.02 for acrolein, 0.07 for 2-methyl-propenal, 0.3 for 2-butenal and 2.0 for 3-methyl-2-butenal [98]. Similar relative reactivities were reported for the hydrogenation of the two latter compounds over Pt(111) and $Pt_{80}Fe_{20}(111)$ single crystals [99]. A theoretical chemistry study demonstrated how the substitution decreases the adsorbability through the C=C bond and thus its reactivity [100].

6.2. Bimetallic and metal–support interaction effects

6.2.1. Hydrogenation of CNB

The liquid-phase hydrogenation of CNB was studied (i) on a series of PtM'/Al_2O_3 catalysts (M′=Sn, Pb, Al, Zn, Ge, Sb) [101], and (ii) on monometallic Pt catalysts supported on Al_2O_3, TiO_2, MgO and ZrO_2 [25]. The main properties are reported in Table 7. The kinetics of the reaction were the same on Pt/Al_2O_3 and on $PtZn/Al_2O_3$. On bimetallic catalysts the TOF went through a maximum value for M′/Pt = 0.1–0.2 (at/at). Such behavior was also reported by Galvagno et al. [102] for nitrobenzene hydrogenation on PtSn/nylon catalysts. They suggested that tin species activate the N=O bond, which became more reactive towards the attack by chemisorbed hydrogen. This point of view is in good agreement with the behavior of Pt/TiO_2(HT) reduced at 773 K (Table 7). The catalyst is in the SMSI state (H/Pt decreased sharply without any great modification of the Pt particle size), which means that TiO_x species have migrated onto the Pt particles [7,53]. The presence of TiO_x adspecies also activates the N=O bond, and the TOF was increased by ten.

The most interesting point deals with the selectivity to CAN which was increased

Table 7
Yield of products for the hydrogenation of CNB at high conversion (>98%) over supported Pt catalysts: $T_R = 303$ K; $C_R = 0.52$ mol dm^{-3}

Sample	M′/Pt (at/at)	H/Pt	d_p (nm)	Conversion (mol%)	Yield of products (mol%)			
					AN	CNSB[a]	CAN	Others[b]
Pt/Al_2O_3	0	1.0	1.1	99.7	16.9	0.19	82.1	0.25
$PtSn/Al_2O_3$	0.11	0.71	1.1	98.6	3.20	0.50	86.6	8.30
$PtSn/Al_2O_3$	0.25	0.64	1.2	99.2	3.30	0.03	94.4	0.60
$PtSn/Al_2O_3$	0.36	0.41	1.3	99.5	1.16	0.03	97.5	0.80
$PtZn/Al_2O_3$	0.54	0.6	1.3	98.6	1.50	—	97.1	—
$PtTiO_2$(LT)[c]	—	0.35	3.2	98.5	0.57	—	97.7	0.26
$PtTiO_2$(HT)[d]	—	0.04	3.0	99.7	0.35	—	99.3	—

[a] CNSB: chloronitrosobenzene.
[b] Azo- and azoxy-dichlorobenzenes.
[c] Reduced at 573 K.
[d] Reduced at 773 K.

upon tin or zinc addition. As developed in the influence of Pt particle size on this reaction, two propositions were postulated for that behavior (*vide supra*). For checking these points, the hydrodechlorination of CAN (Table 8) and its inhibiting effect on the initial rate of CNB hydrogenation (Table 6) were carried out.

Only small changes in the hydrodechlorination rate of CAN were observed upon alloying Pt with Zn (Table 8). By contrast, the inhibiting effect of CAN on the initial rate of CNB hydrogenation was much higher on Pt/Al_2O_3 than on $PtZn/Al_2O_3$ catalyst (Table 6). A threefold decrease of activity was observed on the former, whereas it reached a value of 30 on the latter. In a first approximation we can conclude that the ratio of the adsorption constants $\lambda_{CAN}/\lambda_{CNB}$ is divided by ten when Zn is alloyed to Pt. The decrease of the strength of adsorption of CAN upon alloying Pt with elements possessing an electron donor character suggests that the effect of these promoters of selectivity is to induce a higher electronic density at the Pt sites.

Concerning the promotion observed on Pt/TiO_2 reduced at 773 K, the effect of

Table 8
Reaction rate and TOF for the hydrodechlorination of *p*-chloroaniline over Pt-based catalysts; $T_R = 303$ K, $C_{CAN} = 0.13$ mol dm^{-3}

Sample	H/Pt	d_p (nm)	Rate (mol g^{-1} s^{-1})	TOF (s^{-1})
Pt/Al_2O_3	1.0	1.1	4.0×10^{-6}	0.056
$PtZn/Al_2O_3$	0.6	1.3	3.7×10^{-6}	0.084
Pt/TiO_2(HT)	0.04	3.0	0.11×10^{-6}	0.11

CAN concentration on the initial rate of CNB hydrogenation over Pt/Al_2O_3 and $Pt/TiO_2(HT)$ catalysts is reported in Table 6. It appears that the inhibiting effect of CAN was slightly lower on $Pt/TiO_2(HT)$. A tenfold decrease of activity was observed on the latter, whereas it reached a value of 30 on the former. In a first approximation we can conclude that the ratio of the adsorption constants $\lambda_{CAN}/\lambda_{CNB}$ is divided by three for Pt/TiO_2 in the SMSI state, whereas we found that upon alloying Zn to Pt the $\lambda_{CAN}/\lambda_{CNB}$ ratio was divided by a factor of ten; thereupon, an increase of CAN selectivity from 82.1% to 97.2% occurred (Table 7). In the present case when passing from Pt/Al_2O_3 to $Pt/TiO_2(HT)$ catalysts, the $\lambda_{CAN}/\lambda_{CNB}$ ratio decreased by a factor of three only, but the yield to CAN increased from 82.1% to 99.3%. Therefore, the decrease of CAN adsorption strength was not large enough to account for this result. The rate of CAN hydrodechlorination over Pt/Al_2O_3 and $Pt/TiO_2(HT)$ is reported in Table 8. The relative reactivity between CNB and CAN was much higher on $Pt/TiO_2(HT)$ than Pt/Al_2O_3 (Tables 6 and 8). Very probably, this is the key factor responsible for the enhancement of CAN yield on $Pt/TiO_2(HT)$. In this respect, the behavior of $Pt/TiO_2(HT)$ differs from $PtZn/Al_2O_3$, for which the high CAN yield came mainly from the lower CAN adsorption strength. As said above, this high reactivity toward the N=O bond may be the characteristic feature of the mixed sites at the borderline between bare platinum and TiO_x adspecies. A similar activation of the C=O bond by TiO_x adspecies was proposed by Vannice and Sen [103] for the hydrogenation of crotonaldehyde on $Pt/TiO_2(HT)$ in the SMSI state. If we take into account the specific behavior of $Pt/TiO_2(HT)$ we can tentatively propose the reaction site schematically pictured in Scheme 7. The main feature of this site is the adsorption of CNB in part over TiO_x species, which, moreover, accounts for both the low competition between hydrogen and CNB and the high TOF.

6.2.2. *Hydrogenation of CAL*

Recent reviews have highlighted the role and the effects of promoters [104] and of metal–support interaction [105] in the hydrogenation of α,β-unsaturated aldehydes. As a general rule, the TOF and the selectivity to the unsaturated alcohol are

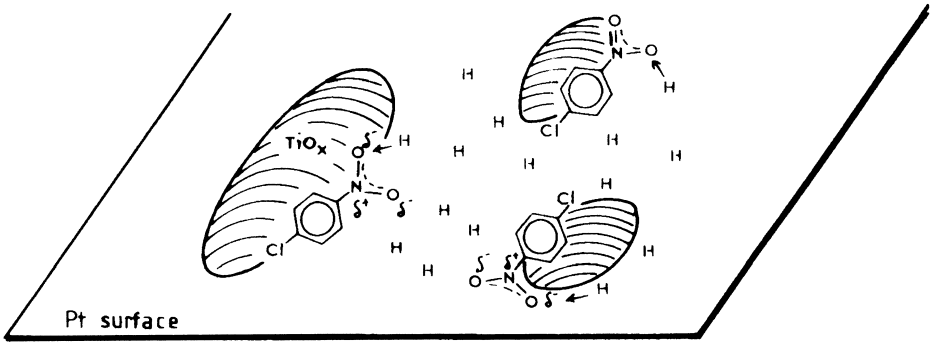

Scheme 7. Reaction sites for CNB hydrogenation on Pt/TiO_2 in the SMSI state.

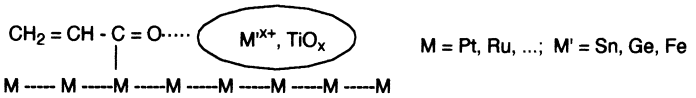

Scheme 8. Reaction sites for hydrogenation of CAL on a metallic-promoted catalyst.

improved when adding Sn, Ge, Fe, etc. to the active transition metal (Pt, Ru, Ni, etc.) and when a partially reducible support, like TiO_2, is used. The promoting action is seen as a strong interaction between the carbonyl group and a positively charged center, i.e. $Fe^{\delta+}$, $Sn^{\delta+}$, $TiO_x^{\delta+}$, pictured in Scheme 8. An attractive feature of the species shown in this scheme is that they cannot be formed from ketones and their existence would explain the large difference in promoter effect of aldehydes and ketones.

A particular case of promotion is observed with the use of a fullerene-based support. This situation will be discussed later.

The liquid-phase hydrogenation of CAL was thus studied: (i) on model RuM'/Al_2O_3 (M′=Sn, Fe, Zn, etc.) prepared by controlled surface reaction (Section 3.2) from a parent Ru/Al_2O_3 [95]; (ii) on RuM'/ZrO_2 (M′=Sn, Fe) prepared in the same way [106]; on a carbon-nanotubes-supported Ru material [107]; (iv) on a Pt catalyst supported on silica chemically grafted with [60]fullerene [108]. Table 9 presents the data obtained on some of these various catalysts.

The selectivity to COL increased until 50–70% of CAL conversion, whatever the catalyst. This is due to hydrocinnamaldehyde (HCAL) formed at the beginning of the reaction, probably by a geometric action [93,95,96]. The TOF increased by a factor of 2–6 upon addition of the second metal. This promotion in activity, in full agreement with previous reports [4,104,105], comes from the polarization of the C=O bond, thus promoting its attack by adsorbed H atoms (*vide supra*). The initial selectivity (at zero conversion) to COL was also improved with the "bimetallic"

Table 9
Catalytic properties of supported metal catalysts for the hydrogenation of CAL at 383 K; $C_{CAL}=7.9\times10^{-4}$ mol cm^{-3}, $P(H_2)=4.5$ MPa

Catalyst	M′/Ru (at/at)	H/Ru (Pt)	dp (nm)	TOF (h^{-1})	Selectivity to COL at increasing CAL conversion (mol%)		
					0	25	50
Ru/Al_2O_3	—	0.60	1.9	1.48	22.0	55.0	52.0
$RuSn/Al_2O_3$	0.20	0.20	2.1	7.13	46.8	60.0	63.6
Ru/TiO2(HT)[a]	—	0.04	1.25	23.0	55.0	69.0	74.0
Ru/ZrO_2	—	0.80	2.1	84	52.0	61.0	61.0
$RuSn/ZrO_2$	0.53	0.45	2.2	76	66.0	72.5	75.5
$RuFe/ZrO_2$	0.15	0.52	—	135	52.0	55.0	55.0
Ru/C-nanotubes	—	0.30	3.5	—	84.0	90.0	92.0
Pt/SiO_2–C_{60}	—	0.36	—	—	80.0	85.0	88.0

[a] Reaction temperature: 333 K.

catalysts. However, these high values of initial selectivity were not sustained at high CAL conversion. Based on this, we suggested that the addition of the second element to Ru produces the same effect on initial selectivity as the adsorption of HCAL. That is, the hindering of CAL adsorption as a flat species by the chemisorbed HCAL.

When compared with an Ru/Al_2O_3 of a similar particle size, the Ru/TiO_2 and Ru/ZrO_2 catalysts behaved differently. These catalysts showed much higher selectivity than might be expected. Indeed, the high temperature reduced Ru/TiO_2(HT) shows features characteristic of SMSI, a sharp decrease of hydrogen uptake, from 0.87 to 0.04 after reduction at 773 K, without any sintering of the metallic phase, due to the migration of TiO_x adspecies onto the Ru particles [7,53]. The TOF at 333 K on Ru/TiO_2(HT) was higher than on Ru/Al_2O_3 at 383 K, thanks to the strong polarization of the C=O bond by electron-withdrawing TiO_x species. The initial selectivity to COL was high and culminated at 74% at 50% CAL conversion.

The Ru/ZrO_2 catalyst shows interesting behavior. In terms of selectivity to COL, the catalyst behaved in a manner similar to Ru/TiO_2(HT), and this was also true for acrolein hydrogenation [94]. However, the catalysts composed of very small Ru particles did not enter the SMSI state. We proposed the occurrence of specific sites at the periphery of the Ru particles. From temperature-programmed reduction [106], it appeared that ZrO_2 was partially reduced, probably at the boundary with Ru particles. These Ru–ZrO_x mixed sites would reproduce, in part, the behavior of Ru/TiO_2. The CAL molecule will be bonded on the sites through the C=O bond and Zr^{x+} species. The infra-red spectroscopy of adsorbed CO provided evidence of bridged CO species bonded at the borderline of Ru^0 particles through the C atom but also bridge-bonded to the coordinatively unsaturated Zr^{4+} or Zr^{3+} ions through the O atom [106]. Such a species was proposed to give a broad CO absorption band occurring at ca. 1850 cm^{-1}. The low C–O stretching frequency of this adsorbed CO species is evidence of a weaker CO bond. Wagray et al. [109] reported a similar broad band around 1900–2000 cm^{-1} when studying CO adsorption on an RuK^+/SiO_2 catalyst. They concluded that a strong interaction occurred between CO and K^+. The addition of Sn to the Ru/ZrO_2 catalyst even resulted in an additional improvement of COL selectivity, which peaked at 75.5% at 50% COL conversion (Table 9) [106].

Fairly high selectivity to COL was obtained on Ru supported on carbon nanotubes, reaching 92% at 50% conversion [107]. The carbon nanotubes were prepared by the arc discharge technique and were mainly constituted of tubes from 4 to 30 nm in diameter and up to 1 μm in length. The Ru particles, from 2 to 7 nm, were supported on the outer shells of the tubes.

On the other hand, we have prepared an organic–inorganic hybrid material composed of SiO_2 chemically grafted with [60]fullerene [110]. Pt particles were supported on the one-dimensional layer of grafted [60]fullerene. This material, tested in the hydrogenation of CAL, exhibited fairly high selectivity to COL: 89% at 80% CAL conversion [108]. This behavior was assigned to a joint adsorption of CAL on both [60]fullerene and Pt particles at their borderline. In this picture, the phenyl ring will be attracted by [60]fullerene, thus favoring an orientation of the α,β-unsaturated system for an adsorption by the C=O on the Pt particles.

7. Concluding remarks

It has been known for some time that great changes in the orientation of the reaction could be reached in the conversion of alkanes by tuning the superficial structure of metal particles. This is due to the very wide diversity of intermediates which can be accommodated by the surface depending on the alkane and the coordination of the metal site. The same approach is now going on in some hydrogenations of polyfunctional organic compounds, and would fruitfully apply to the design of intrinsically selective metallic catalysts without the help of promoters added in the reaction medium. Research into new bimetallic formulations and in metal–support interaction seems particularly attractive for this aim.

References

[1] M. Boudart, A. Aldag, J.E. Benson, N.A. Dougharty, C. Harkins Girvin, J. Catal. 6 (1966) 92.
[2] M. Boudart, Adv. Catal. 20 (1969) 153.
[3] H.S. Taylor, Proc. R. Soc. London Ser. A: 108 (1925) 105.
[4] V. Ponec, G. C. Bond, In: Catalysis by Metals and Alloys, Elsevier, Amsterdam, 1995.
[5] M. Che, C.O. Bennett, Adv. Catal. 36 (1989) 55.
[6] V. Ponec, Adv. Catal. 32 (1983) 149.
[7] G.L. Haller, D.E. Resasco, Adv. Catal. 36 (1989) 173.
[8] G.A. Somorjai, Langmuir 7 (1991) 3176.
[9] G.C. Bond, Acc. Chem. Res. 26 (1993) 490.
[10] G.C. Bond, Chem. Soc. Rev. 20 (1991) 441.
[11] P. Sabatier, in: C. Béranger (Ed.) La Catalyse en Chimie Organique, La Libraire Polytechnique Paris, 1913.
[12] N.I. Kobozev, Acta Physicochim. URSS 9 (1938) 1.
[13] O.M. Boronin, V.S. Poltorak, Int. Chem. Eng. 7 (1967) 452.
[14] R. van Hardeveld, F. Hartog, Surf. Sci. 15 (1969) 189.
[15] W.M.H. Sachtler, R.A. van Santen, Adv. Catal. 26 (1977) 69.
[16] R. Coekelbergs, A. Frennet, G. Lienard, P. Resibois, J. Phys. Chem. 39 (1963) 604.
[17] J.A. Dalmon, G.A. Martin, J. Catal. 66 (1980) 214.
[18] L. Guczi, A. Sarkany, Catalysis Special Periodic Report, The Chemical Society, London, 1995, p. 318.
[19] J.P. Boitiaux, J. Cosyns, S. Vasudevan, Stud. Surf. Sci. Catal. 16 (1982) 123.
[20] B. Coq, R. Dutartre, F. Figueras, T. Tazi, J. Catal. 122 (1990) 438.
[21] B. Coq, A. Bittar, F. Figueras, Appl. Catal. 59 (1990) 103.
[22] B. Coq, E. Crabb, M. Warawdekar, G.C. Bond, J.C. Slaa, S. Galvagno, L. Mercadante, J. Garcia Ruiz, C. Sanchez Sierra, J. Mol. Catal. 92 (1994) 107.
[23] B. Coq, P.S. Kumbhar, C. Moreau, P. Moreau, F. Figuéras, J. Phys. Chem. 98 (1994) 10180.
[24] B. Coq, A. Chaqroune, F. Figueras, B. Nciri, Appl. Catal. 82 (1992) 231.
[25] B. Coq, A. Tijani, R. Dutartre, F. Figuéras, J. Mol. Catal. 79 (1993) 253.
[26] C. Travers, T.D. Chan, R. Snappes, J.P. Bournonville, US Patent 4 456 775, 1984.
[27] H.G. Aduriz, P. Bodnariuk, B. Coq, F. Figuéras, J. Catal. 119 (1989) 97.
[28] B. Coq, A. Goursot, T. Tazi, F. Figuéras, D. Salahub, J. Am. Chem. Soc. 113 (1991) 1485.
[29] B. Coq, A. Bittar, R. Dutartre, F. Figuéras, J. Catal. 128 (1991) 275.
[30] G.C. Bond, J.C. Slaa, J. Mol. Catal. 89 (1994) 221.
[31] J.R. Anderson, Adv. Catal. 23 (1973) 1.

[32] Z. Paal, P. Tetenyi, Catalysis Special Periodic Report, Vol. 5, The Chemical Society, London, 1982, p. 80.
[33] F.G. Gault, Adv. Catal. 30 (1980) 1.
[34] G. Leclercq, R. Maurel, J. Catal. 50 (1977) 87.
[35] G. Leclercq, R. Maurel, Bull. Soc. Chim. Belg. 88 (1979) 599.
[36] G. Leclercq, S. Pietrzik, M. Peyrovi, M. Karroua, J. Catal. 99 (1986) 1.
[37] T. Stace, Nature 331 (1988) 116.
[38] B. Coq, F. Figuéras, J. Mol. Catal. 40 (1987) 93.
[39] B. Coq, E. Crabb, F. Figuéras, J. Mol. Catal. A: 96 (1995) 35.
[40] B. Coq, T. Tazi, R. Dutartre, F. Figuéras, in: New Frontier in Catalysis, Proc. 10th Int. Congr. Catalysis, Akademiai Kiado, Budapest, 1993, Vol. C, p. 2367.
[41] J.K.A. Clarke, A.C.M. Creaner, Ind. Chem. Prod. Res. Dev. 20 (1981) 574.
[42] J.J. Burton, E. Hyman, D.G. Fedak, J. Catal. 37 (1975) 106.
[43] V.S. Sundaram, P. Wynblatt, Surf. Sci. 52 (1975) 569.
[44] J.K. Strohl, T.S. King, J. Catal. 116 (1989) 540.
[45] M.C. Sanchez, J. Garcia, M.G. Proietti, J. Blasco, J. Mol. Catal. A: 96 (1995) 65.
[46] A. Goursot, L. Pedocchi, B. Coq, J. Phys. Chem. 98 (1994) 8747.
[47] A. Goursot, L. Pedocchi, B. Coq, J. Phys. Chem. 99 (1995) 12718.
[48] A. Goursot, B. Coq, L.C. de Ménorval, T. Tazi, F. Figuéras, D.R. Salahub, Z. Phys. D: 19 (1991) 367.
[49] L.C. de Ménorval, A. Chaqroune, B. Coq, F. Figuéras, J. Chem. Soc. Faraday Trans. 93 (1997) 3715.
[50] G. del Angel, B. Coq, F. Figuéras, J. Catal. 95 (1985) 167.
[51] B. Coq, R. Dutartre, F. Figuéras, A. Rouco, J. Phys. Chem. 93 (1989) 4904.
[52] M.W. Smale, T.S. King, J. Catal. 125 (1990) 335.
[53] S.J. Tauster, S.C. Fung, J. Catal. 55 (1978) 59.
[54] B. Coq, A. Bittar, R. Dutartre, F. Figuéras, Appl. Catal. 60 (1990) 33.
[55] G.C. Bond, B. Coq, R. Dutartre, J. Garcia, A.H. Hooper, M.G. Proietti, M. Conception Garcia, J.C. Slaa, J. Catal. 161 (1996) 480.
[56] S. Gao, L.D. Schmidt, J. Catal. 115 (1989) 356.
[57] M.J. Molina, F.S. Rowland, Nature 249 (1974) 810.
[58] A. Wiersma, E.J.A.X. van de Sandt, M. Makkee, H. van Bekkum, J.A. Moulijn, Curr. Top. Catal. in press.
[59] L.E. Manzer, V.N. Mallikarjuna Rao, Adv. Catal. 39 (1992) 329.
[60] J.A. Rabo, in: New Frontier in Catalysis, Proc. 10th Int. Congr. Catalysis, Akademiai Kiado, Budapest, 1993, Vol. A, p. 1.
[61] I. Dodgson, Stud. Surf. Sci. Catal. 78 (1993) 1.
[62] C. Gervasutti, L. Marangoni, W. Parra, J. Fluorine Chem. 19 (1981) 1.
[63] B. Coq, J.M. Cognion, F. Figuéras, D. Tournigant, J. Catal. 141 (1993) 21.
[64] A. Wiersma, E.J.A.X. van de Sandt, M. Makke, C.P. Luteijn, H. van Bekkum, J.A. Moulijn, Catal. Today 27 (1996) 257.
[65] Z. Karpinski, K. Early, J.L. d'Itri, J. Catal. 164 (1996) 378.
[66] W. Juszczyk, A. Malinowski, Z. Karpinski, Appl. Catal. in press.
[67] E.D. Boyes, D.R. Coulson, G.W. Coulson, M.P. Diebold, P.L. Dai, G.A. Jones, C.S. Kellner, J.J. Lerou, L.E. Manzer, V.N. Mallikarjuna Rao, Proc. EUROPACAT-I Congress, Montpellier, 1993, p. 645.
[68] S. Deshmukh, Z. Karpinski, K. Early, F. Lonyi, J.L. d'Itri, Proc. EUROPACAT-III Congress, Krakow, 1997, p. 358.
[69] B. Coq, G. Ferrat, F. Figuéras, J. Catal. 101 (1986) 434.
[70] R.J. Harper, C. Kemball, Trans. Faraday Soc. 65 (1969) 2224.
[71] P. Mars, D.W. van Krevelen, Chem. Eng. Sci. 3 (1954) 41.
[72] P. Bodnariuk, B. Coq, G. Ferrat, F. Figuéras, J. Catal. 116 (1989) 459.
[73] M. Kraus, V. Bazant, in: Catalysis, Vol. 2, Elsevier, New York, p. 1073.
[74] R.B. LaPierre, L. Guczi, W.L. Kranich, A.H. Weiss, J. Catal. 52 (1978) 230.

[75] F.H. Ribeiro, C.A. Gerken, G.A. Somorjai, C.S. Kellner, G.W. Coulston, L.E. Manzer, L. Abrams, Catal. Lett. 45 (1997) 101.
[76] J.E. Germain, Intra-Sci. Chem. Rep. 6 (1972).
[77] B. Coq, F. Bouchara, D. Tournigant, F. Figuéras, Proc. 1st World Conf. Environmental Catalysis, Pise, 1995, p. 583.
[78] A.H. Weiss, B.S. Gambhir, R.B. Leon, J. Catal. 22 (1971) 245.
[79] B. Coq, F. Figuéras, S. Hub, D. Tournigant, J. Phys. Chem. 99 (1995) 11159.
[80] H.C. Choi, S.H. Choi, O.B. Yang, K.H. Lee, J.S. Lee, Y.G. Kim, J. Catal. 161 (1996) 790.
[81] H.C. Choi, S.H. Choi, O.B. Yang, J.S. Lee, K.H. Lee, Y.G. Kim, J. Catal. 166 (1997) 284.
[82] W.F. Tuley, R.J. Adams, J. Am. Chem. Soc. 45 (1925) 3061.
[83] R.E. Malz Jr. (Ed.), Catalysis of Organic Reaction, Marcel Dekker, New York, 1996.
[84] H.U. Blaser, A. Baiker, R. Prins (Eds.), Heterogeneous Catalysis and Fine Chemical IV, Elsevier, Amsterdam, 1997.
[85] P.N. Rylander, Catalytic Hydrogenation in Organic Syntheses, Academic Press, New York, 1979.
[86] L. Cerveny, I. Paseka, V. Stuckly, V. Ruzicka, Coll. Czech. Chem. Commun. 47 (1982) 853.
[87] G. Carturan, G. Facchin, G. Cocco, G. Navazio, G. Gubitosa, J. Catal. 82 (1983) 56.
[88] B. Coq, A. Tijani, F. Figuéras, J. Mol. Catal. 68 (1991) 331.
[89] A. Tijani, B. Coq, F. Figuéras, Appl. Catal. 76 (1991) 255.
[90] B. Gordon, F. Cyrot-Lackmann, M.C. Desjonquières, Surf. Sci. 68 (1977) 359.
[91] S. Galvagno, A. Donato, G. Neri, R. Pietropaolo, Z. Poltarzewski, J. Mol. Catal. 42 (1987) 379.
[92] G. Neri, M.G. Musolino, R. Pietropaolo, S. Galvagno, Proc. EUROPACAT-III Congress, Krakow, 1997, p. 581.
[93] P. Gallezot, A. Giroir-Fendler, D. Richard, in: W. Pascoe (Ed.), Catalysis of Organic Reactions, Marcel Dekker, New York, 1991, p. 1.
[94] B. Coq, F. Figuéras, P. Geneste, C. Moreau, P. Moreau, M.G. Warawdekar, J. Mol. Catal. 78 (1993) 211.
[95] B. Coq, P.S. Khumbar, C. Moreau, P. Moreau, M.G. Warawdekar, J. Mol. Catal. 85 (1993) 215.
[96] S. Galvagno, G. Capanelli, G. Neri, A. Donato, R. Pietropaolo, J. Mol. Catal. 64 (1991) 237.
[97] S. Galvagno, C. Milone, A. Donato, G. Neri, R. Pietropaolo, Catal. Lett. 18 (1993) 349.
[98] B. Coq, F. Figuéras, C. Moreau, P. Moreau, M.G. Warawdekar, Catal. Lett. 22 (1993) 189.
[99] P. Beccat, J.C. Bertolini, Y. Gauthier, J. Massardier, P. Ruiz, J. Catal. 126 (1990) 451.
[100] F. Delbecq, P. Sautet, J. Catal. 152 (1995) 217.
[101] B. Coq, A. Tijani, F. Figuéras, J. Mol. Catal. 71 (1992) 317.
[102] S. Galvagno, A. Donato, G. Neri, R. Pietropaolo, J. Mol. Catal. 42 (1987) 379.
[103] M.A. Vannice, B. Sen, J. Catal. 115 (1989) 65.
[104] V. Ponec, Appl. Catal. A: 149 (1997) 27.
[105] A.B. da Silva, E. Jordao, M.J. Mendes, P. Fouilloux, Appl. Catal. A: 148 (1997) 253.
[106] B. Coq, P.S. Khumbar, C. Moreau, P. Moreau, F. Figuéras, J. Phys. Chem. 98 (1994) 10180.
[107] J.M. Planeix, N. Coustel, B. Coq, V. Brotons, P.S. Khumbar, R. Dutartre, P. Geneste, P. Bernier, P.M. Ajayan, J. Am. Chem. Soc. 116 (1994) 7935.
[108] B. Coq, V. Brotons, J.M. Planeix, L.C. de Menorval, R. Dutartre, J. Catal. in press.
[109] A. Wagray, J. Wang, R. Oukaci, D. Blackmond, J. Phys. Chem. 96 (1992) 5964.
[110] J.M. Planeix, B. Coq, L.C. de Menorval, P. Medina, J. Chem. Soc. Chem Commun. (1996) 2087.